View metadata, citation and similar papers at core.ac.uk
brought to you by CORE
provided by Lodz University of Technology Repository

BUCKLING AND POST-BUCKLING BEHAVIOUR OF CHANNEL-SECTION COMPOSITE COLUMNS WITH VARIOUS SEQUENCES OF PLIES

H. DĘBSKI
Department of Machine Design, Lublin University of Technology
Nadbystrzycka 36, 20-618 Lublin, Poland

T. KUBIAK
Department of Strength of Materials, Lodz University of Technology
Stefanowskiego 1/15, 90-924 Łódź, Poland

A. TETER
Department of Applied Mechanics, Lublin University of Technology
Nadbystrzycka 36, 20–618 Lublin, Poland

The paper deals with buckling of thin-walled channel-section composite columns subjected to static compression. It was assumed, that the columns were simply supported at both ends. For experimental testing three series of specimens were manufactured with autoclaving technique. The specimens had identical dimensions but differed about ply sequence. The Hexcel's HexPly M12 carbon-epoxy prepreg was used in order to fabricate the channel-section columns. During the stand tests minimal critical forces and the corresponding buckling modes were determined with an application of electrical strain gauges. In addition, post-critical equilibrium paths for small overloads (150 % of the critical force) were determined. The experimental results were compared to the ones obtained numerically with the finite element method (FEM).

1. INTRODUCTION

In design process of complex composite materials an important role plays the plies arrangements, having a decisive influence on load carrying abilities of particular components of the stress state. This applies to thin-walled composite structures stability as well, in which a specific ply sequence can have essential influence on a value of critical load or a structure's stiffness in post-critical state [1].

This article presents experimental results of thin-walled composite columns having channel-section subjected to compressive load. It was assumed, that the profiles are simply supported at both ends. The purpose of the conducted research was determination of the ply sequence influence on critical load value and the mode of stability loss of the compressed columns. Moreover, an attempt to assess the influence of the ply sequence on the structure's stiffness in post-critical state was made. The obtained experimental results allowed to verify numerical calculations performed with the finite element method (FEM) using the Abaqus software.

2. SUBJECT AND SCOPE OF RESEARCH

The experiments were performed on thin-walled composite columns channel-section. The columns were made of the M12/35%/UD134/AS7/300 carbon-epoxy unidirectional prepreg tape (HexPly, Hexcel**).** The composite's matrix was epoxy resin (mass density: ρ=1.24 g/cm^3; mechanical characteristics: R_m=64 MPa; ν=0.4; E=5.1 GPa), whereas the reinforcement were the AS7J12K carbon fibres (ρ= 2.5 g/cm^3, R_m=4830 MPa; ν=0.269; E=241 GPa). Test specimens were manufactured with autoclaving technique, providing high strength of the fabricated structures, as well as repeatability of the production process [2]. Three types of 8-ply composite columns were tested. The layups were symmetrical, as follows: (a) - $[0,-45,45,90]_s$, (b) - $[0,90,0,90]_s$, (c) - $[45,-45,90,0]_s$. Each ply had the same thickness of 0.131 mm. In Fig. 1 the dimensions of the profiles and an exemplary ply sequence were given.

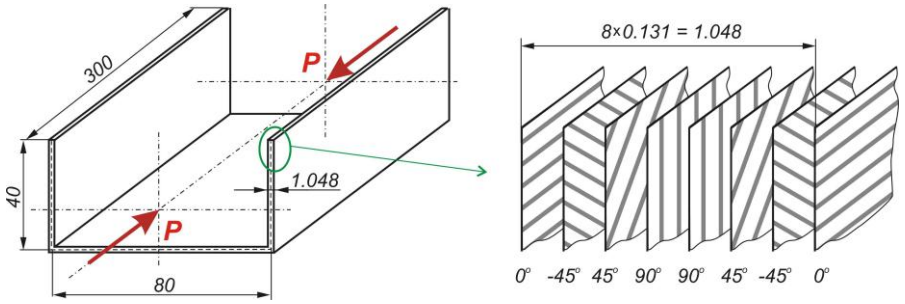

Fig. 1. Dimensions and exemplary plies arrangement for column under analysis

For the used composite prepregs the following mechanical characteristics were determined experimentally - Young's moduli: E_1 = 130.71 GPa, E_2 = 6.36 GPa, Kirchhoff's modulus: G_{12} = 4.18 GPa, Poisson's ratio: ν_{12} = 0.32. In destructive tests the following features were additionally estimated: tensile strength in the 0^o direction (longitudinal): σ_{M1}=1867.2 MPa and in perpendicular 90^o direction σ_{M2}=2597 MPa; shearing strength for the ±45° direction: τ_{12M}=100.15 MPa and compressive strength in the two perpendicular 0º and 90º directions: σ_{cM1}=1531 MPa and σ_{cM2}=214 MPa, respectively. The experimentally determined strength characteristics of the carbon-epoxy composite were exploited in the definition of material model in the FEM calculations.

The manufactured composite columns underwent texture quality control of the laminate with non-destructive testing (NDT) methods and microstructural inspection considering a localization of possible flaw. The flaw can have a form of delamination or porosity cluster. They are the most frequently occurring laminate defects and can seriously deteriorate the material strength. Moreover, they can be sources of failure of the composite structure. The NDT tests were done with OmniScan MXU-M ultrasonic defectoscope, equipped with Olympus 5L64 A12 measurement head. The walls of all the produced profiles were inspected considering flaw identification. The A-scan and the B-scan techniques were used, as they allowed to localize and to dimension the possible flaw within the material. Additionally, microstructural research was lead with X-ray micro-

tomography (SkyScan 1174 microtomograph) and with optical microscopy (Nikon MA200). Both techniques employed computer-assisted image analysis (Image Pro Plus, NIS-Elements). These methods enabled additional analysis of the composite profiles round corners' radii, where a possibility of discontinuity in the form of interlayer delamination was particularly high. The performed measurement confirmed very good quality of the manufactured composite profiles, as no internal flaws were detected.

3. NUMERICAL CALCULATIONS

The numerical calculations were performed with the FEM using the Abaqus software. The scope of the calculations covered critical state analysis – linear calculations with the *buckling analysis* option, enabling determination of critical loads and the columns' buckling modes. Next stage of computations was a non-linear analysis of a structure with implemented imperfections related to the first buckling mode. This enabled observation of post-critical deformation. In non-linear calculations the Newton-Raphson incremental-iterative method was employed [3]. In the process of the structure discretization the S4R, i.e. 4-node shell elements with linear shape function and reduced integration having 6 degrees of freedom at each node were used. A numerical model of the channel-section composite columns is presented in Fig. 2.

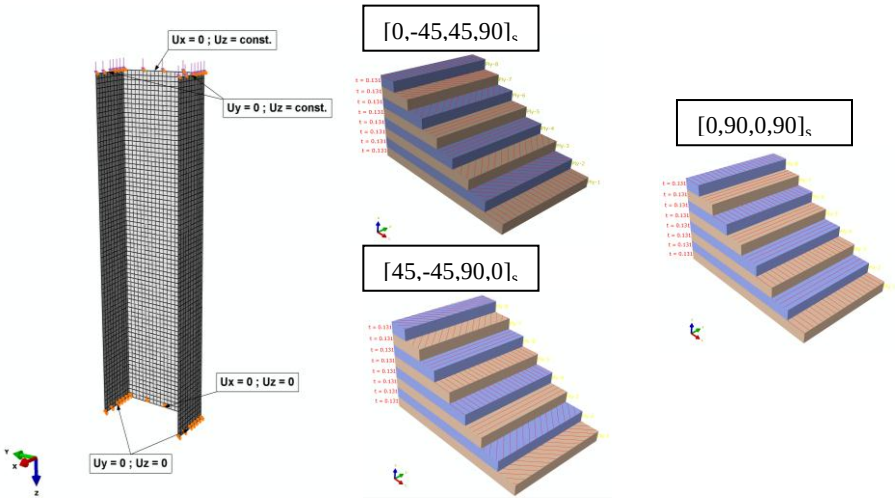

Fig. 2. FEM model of the tested composite columns

The scope of numerical simulations covered also an attempt to assess the possibility of damage occurrence in the composite in post-critical range. An assessment of material effort, as well as an estimation of the failure load level was done with the Tsai-Wu criterion [4], using the experimentally determined limit parameters of the composite. In addition, a assumed FEM model validations was done with the analytical-numerical (A-N) method [5-7], based on the Koiter theory [8].

4. EXPERIMENTS

The experimental tests consisted of axial compression of the composite columns within a range from 0 up to ca 150 % of the critical load. In order to provide fine axial loading conditions, special self-aligning grips with spherical bearings were designed and fabricated. The grips transfered the load exerted with the Zwick Z100/SN3A universal testing machine to a specimen - Fig. 3. The used machine is in accuracy class 1. Any imperfections of the columns' ends, able to cause unwanted boundary effects, were compensated by specially prepared soft-plastic pads.

Fig. 3. Stand test with self-aligning grips for compressive loading of composite columns

On the specimen's internal and external surfaces in the vicinity of the biggest web's deflection area Vishay's electrical strain gauges were sticked along the loading direction. The two CEA-06-125UW-350 series gauges had a constant k=2.135±0.5 % and electrical resistance of 350 Ω±0.3 %. In addition the deflections were measured with the optoNCDT 1605 laser dilatometer. All the measurement elements were plugged to the MGCplus system (Hottinger). During the tests the indications of all sensors were registered with a frequency of 1 Hz. It is worth underlining, that no symptoms of the columns' failure were noticed during the tests. Before each test the loading setup was pre-loaded up to 25 % of the expected critical load in order to provide the best possible alignment of the column and the grips. Next, the retainers were removed and the specimen was unloaded to 0. All tests were conducted in standard conditions, at 23^{o}C with constant velocity of the cross-bar equal to 1 mm/min. The experiments were lead in sub-critical range with registration of parameters needed in determination of critical loads, as well as in post-critical range. For each of the considered ply sequences three samples were tested and the measurements were done thrice. Thus, nine measurements were performed for each layup in order to determine the columns' sub- and post-critical characteristics.

On the basis of the obtained experimental results the values of critical load were determined, in accordance with the following merthods [9-18]:
- the mean-strain (P-ε_{sr}) method – denoted as K1 [9,12,17],
- the method of straight-lines intersection in the plot of mean strains – denoted as K2 [9,12,17],
- the P-$(\varepsilon_1 - \varepsilon_2)^2$ –method – denoted as K3 [11,17],
- the P-$(\varepsilon_1 - \varepsilon_2)$-curve inflection point method - denoted as K4 [9].

Preliminary tests showed, that the oldest and the most known Soutwell method [13-18] could not be used, because the values of critical forces manifested big error and, additionally, were not repeatable.

In the mean-strain (P-ε_{sr}) method (K1) two strain gauges were placed along loading direction on both sides of a the web near the biggest-deflection area. Next the values of strains: ε_1 and ε_2 were measured with gauges and registered as a function of the compressive force P. In the end the mean strains were calculated. Construction of the P-ε_{sr} plot enabled determination of the critical forces – just reading an ordinate of the point, in which vertical tangent line touched the plot curve. The method of straight-lines intersection in the plot of mean strains (K2) was similar to the above described K1 method. The only difference was the way of critical force readout. For the purpose of critical loads determination it was necessary to approximate both pre- and post buckling state of the ε_{sr}-P plot with straight lines. The critical state was determined as an ordinate of intersection point of these straight lines. In the P-$(\varepsilon_1 - \varepsilon_2)^2$ (K3) method a plot of force vs square of deflection had to be constructed. It was a straight line intersecting the load axis at the point of critical force. It is worth noting, that knowing the indications of gauges sticked to the opposite sides of each profile's web one could assume that the relation of the deflection w was directly proportional to the difference of the gauges' indications (ε_1-ε_2). In the last method (K4) for the relation ($\varepsilon_1 - \varepsilon_2$)-$P$ the critical force was determined as an intersection-point ordinate of that curve.

5. RESULTS - DISCUSSION

Both prebuckling and critical states research proved, that the lowest values of the critical loads refered to local modes of stability loss in case of of all the tested composite columns and the respective buckling modes, as well. Fig. 4 presents the lowest buckling modes obtained with numerical calculations (FEM) and in experiments.

A collection of mean values of critical loads and their scatters determined experimentally and comparative values obtained numerically both with the FEM and the A-N method were presented in Fig. 5.

The results shown in Fig. 4 and Fig. 5 indicate both qualitative and quantitative convergence of the buckling modes and the critical load values obtained numerically with the two computational methods and in the experiments. Analysis of the critical loads obtained for all the tested columns with the FEM and the A-N method leads to a conclusion, that the results were practically the same – the biggest divergences of ca 4.3% were obtained for the profile with the $[0,-45,45,90]_s$ layup. Moreover, on the basis of the plot in Fig. 4 one can conclude, that numerical results place usually in the middle of the critical load range determined with particular methods exploiting the experimental data. The only exception was the $[45,-45,90,0]_s$ profile, for which the computational value of critical force was for 6 % lower than the experimental one.

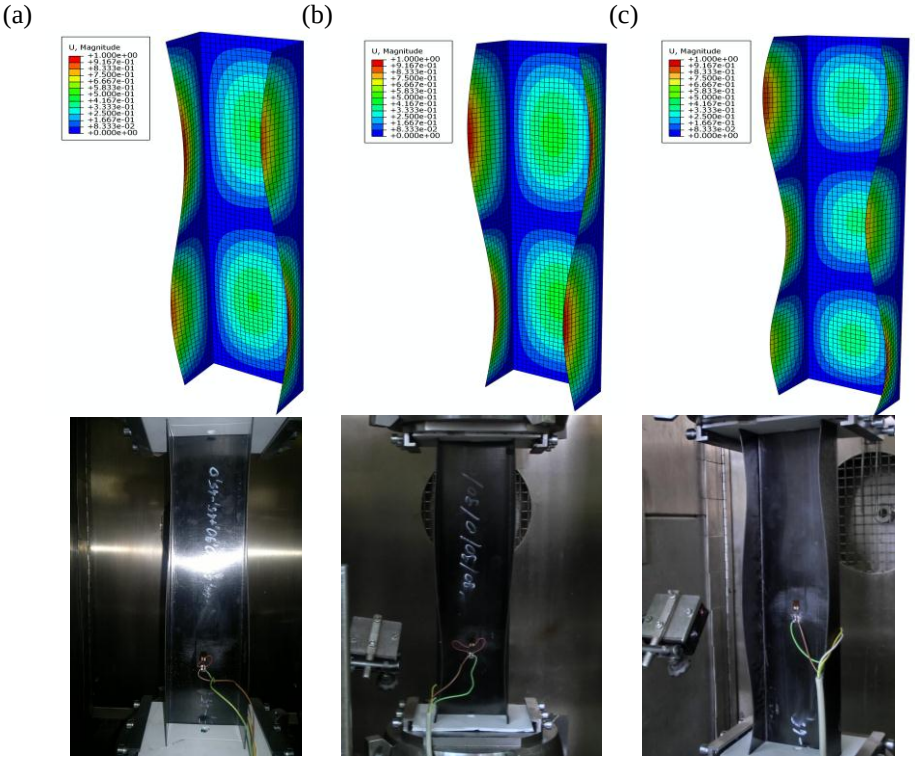

Fig. 4. Buckling modes of the composite columns:
(a) $[0,-45,45,90]_s$, (b) $[0,90,0,90]_s$, (c) $[45,-45,90,0]_s$

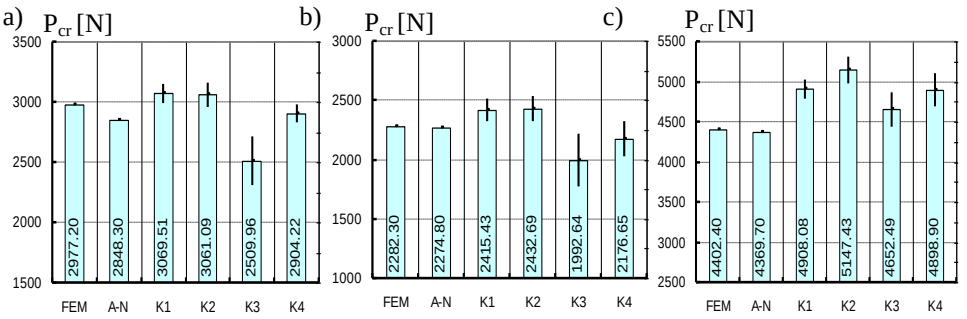

Fig. 5. The mean values of critical forces obtained expeimentally and their scatters for the respective series of samples: (a) $[0,-45,45,90]_s$, (b) $[0,90,0,90]_s$, (c) $[45,-45,90,0]_s$

These results allowed to estimate the influence of the composite layup on critical load values. The smallest values of critical forces were gained in case of the $[0,90,0,90]_s$ profile, whereas the biggest ones - for the $[45,-45,90,0]_s$ ply sequence. On the basis of the performed analyses a columns' tendency to have higher critical load for the layups in which the 0^o-plies were located in the vicinity of the mid-plane. No increase in critical

load among profiles differing only with the location of the 0^o- degrees ply (i.e.: $[0,-45,45,90]_s$ and $[45,-45,90,0]_s$) in comparison to a layup experiencing lower critical load was ca 48 %.

Post-critical range analysis enabled to assess the deformation and the stiffness of the structure after the stability loss in relation to the laminate's plies arrangements. The failure loads were determined only in numerical way using FEM because the experimental tests were lead within the range exceeding ca. 1.5-times. An attempt was made to assess the failure load value in accordance with the Tsai-Wu criterion [4]. In Fig. 6 the post-critical deformation of the compressed columns corresponding to the failure load value was presented (the Tsai-Wu-criterion failure parameter equal to 1).

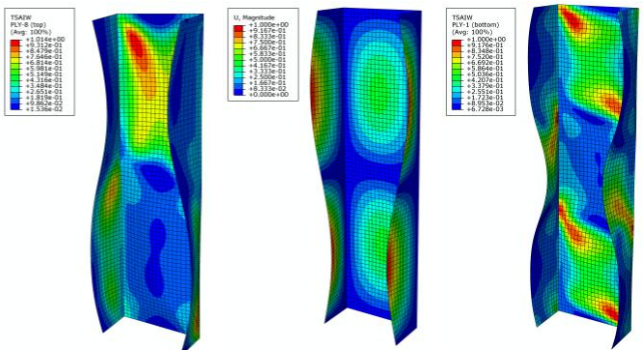

Fig. 6. Post-critical deformation state: (a) $[0,-45,45,90]_s$, (b) $[0,90,0,90]_s$, (c) $[45,-45,90,0]_s$

Zones, where the critical value of the failure parameter was reached indicated the areas endangered to damage occurrence in the laminate's external plies. The values of failure load determined with the FEM in relation to the critical load were collected in Table 1.

The obtained FEM results of the destructive forces showed, that the change of the 0º-plies locations (i.e.: $[0,-45,45,90]_s$ and $[45,-45,90,0]_s$) in relation to the system having lower loading was ca 39 %. This means, the difference in failure load was lower than in critical loads. Interesting results of the critical and failure loads were obtained for the composites with $[0,-45,45,90]_s$ and $[0,90,0,90]_s$ plies sequences. Note, that the critical load in case of the $[0,-45,45,90]_s$ sequence was bigger than the critical force for the $[0,90,0,90]_s$ ply sequence. On contrary, in case of failure loads an opposite tendency was observed. This probably was a result of multiplication of the 0^o- plies number.

Moreover, it should be noted, that among the analysed layups the cross-ply laminate showed the biggest increase in failure force in relation to critical force – ca six times.

Table 1. Failure load values (FEM)

Composite layup	(a) - $[0,-45,45,90]_s$	(b) - $[0,90,0,90]_s$	(c) - $[45,-45,90,0]_s$
Critical force P_{cr} [N]	2977.2	2282.3	4402.4
Failure force P_f [N]	10100	13693	14087

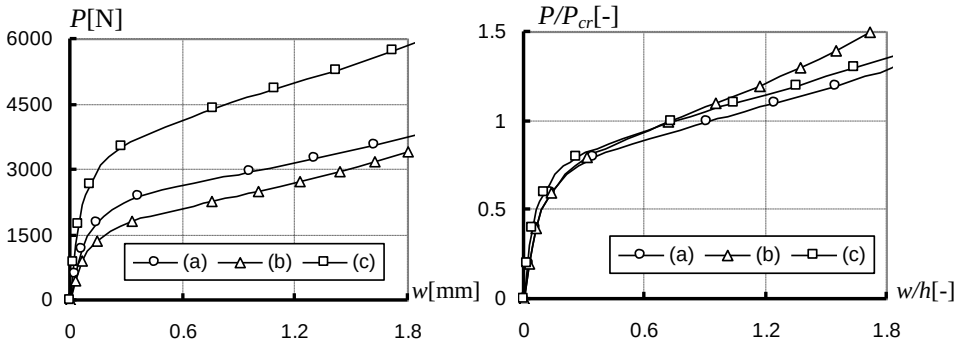

Fig. 7. Comparison of post-critical equilibrium paths for composite columns with different layups: (a) - $[0,-45,45,90]_s$, (b) - $[0,90,0,90]_s$, (c) - $[45,-45,90,0]_s$. obtained with the FEM

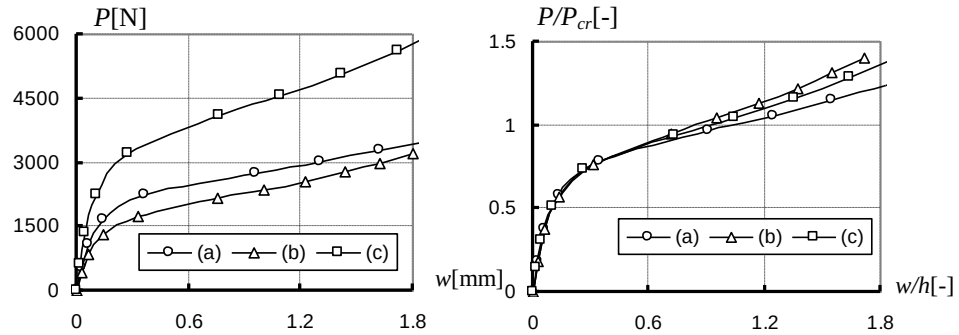

Fig. 8. Comparison of post-critical equilibrium paths for composite columns with different layups: (a) - $[0,-45,45,90]_s$, (b) - $[0,90,0,90]_s$, (c) - $[45,-45,90,0]_s$ obtained with A-N method

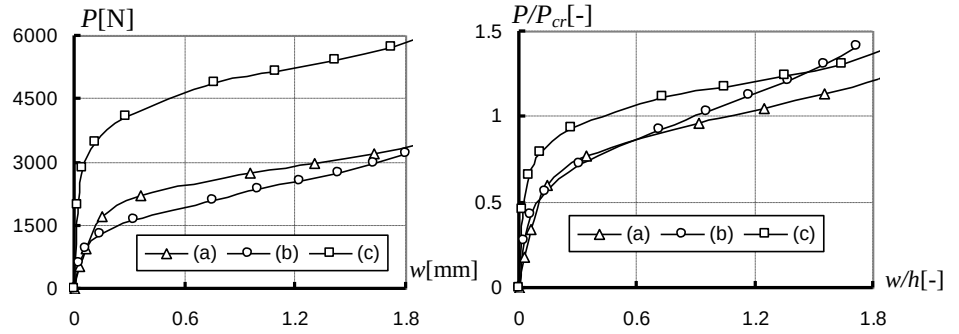

Fig. 9. Comparison of post-critical equilibrium paths for composite columns with different layups: (a) - $[0,-45,45,90]_s$, (b) - $[0,90,0,90]_s$ and (c) - $[45,-45,90,0]_s$ obtained experimentally

Post-critical equilibrium paths were also determined for the nodes experiencing maximal amplitudes of displacement in a slightly post-critical state. Figs 7 ÷ 9 present the results of experiments, as well as the FEM and the A-N method outcomes in both dimensional (*w*-*P*) and non-dimensional coordinate system (w/h-P/P_{cr}, where *h* stands for the columns' wall thickness).

For every tested column high similarity of the computational and the experimental results was gained. However, in the plots the comparison of equilibrium paths was emphasized for different composite's ply-sequences. The comparison of the non-dimensional results obtained with the FEM and the A-N showed that in post-critical state the plies sequence had no influence on the column's stiffness. Namely, the inclination of the curves in post-critical state was very similar. A detailed analysis of the results showed only slightly bigger stiffness of the (c) composite column.

The observations yielding from the dimensional and the non-dimensional plots gained with computational methods were confirmed experimentally – see the similar inclination of the post-critical state curves in Fig. 9. Moreover, it was noticeable, that the deflections of the columns (a) and (b) were bigger than those of the (c) column, when the applied load value was from the post-critical range. The column exhibiting higher critical load deflected less in relation to those having lower critical load.

4. CONCLUSION

In the article the analysis of the thin-walled channel-section composite columns subjected to static compression was presented. The obtained results showed both qualitative and quantitative conformity of buckling modes, as well as values of critical load found by numerical or analytical-numerical calculations with experimental outcomes. Moreover, one could notice, that computational results placed usually in the middle of the critical load range, estimated with particular methods exploiting the experimental results. The obtained outcomes allowed to estimate the influence of the composite's plies sequence on the value of critical load. On the basis of the composite columns behaviour in compression a tendency to have higher critical load was observed, in case of the structures, in which the 0º-plies were located in the vicinity of the layup's symmetry plane. The (b) column exhibited the biggest increase in its failure load in relation to the critical one - even 6 times.

Concerning the stiffness of the considered columns, it was similar for all specimens: the inclination angle of the curves' secant lines was almost the same in post-critical state. Comparison of the deflections of the considered columns lead to a conclusion, that the column (c), having bigger critical load for the applied force from the post-critical range, deformed less than the columns having lower critical loads ((a) and (b)).

ACKNOWLEDGEMENTS

An article written under the ministerial research project no. N N507 241440 The Ministry of Science and Higher Education.

REFERENCES

[1] Swanson S.R., Introduction to Design and Analysis with Advanced Composite Materials, Prentice-Hall, Inc.,1997.

[2] Campbell F.C., Manufacturing Technology for Aerospace Structural Materials, Elsevier 2006.

[3] Abaqus HTML Documentation.

[4] Tsai S.W., Introduction to Composite Materials, Technomic 1980.

[5] Kolakowski Z., Kowal-Michalska K. (eds.), Selected problems of instabilities in composite structures, A Series of Monographs, Technical University of Lodz, 1999.

[6] Teter A., Kolakowski Z., Buckling of thin-walled composite structures with intermediate stiffeners, Composite Structures, 60, 2005, pp.421-428.

[7] Teter A., Kolakowski Z., Lower bound estimation of load-carrying capacity of thin-walled structures with intermediate stiffeners, Thin-Walled Structures, 39(8), 2001, pp. 649-669.

[8] van der Heijden A.M.A. (ed.), W.T. Koiter's Elastic Stability of Solids and Structures, Cambridge University Press, 2009.

[9] Coan J.M., Large-Deflection Theory for Plates With Small Initial Curvature Loaded in Edge Compression, ASME, Journal of Applied Mechanics, Vol. 18, June 1951, pp. 143-151.

[10] Spencer, H.H. andWalker, A.C., Critique of Southwell Plots with Proposals for Alternative Methods, Experimental Mechanics 15(8), 1975, pp.303-310.

[11] Venkataramaiah, K.R., Roorda J., Analysis of local plate buckling experimental data, Sixth International Specialty Conference on Cold-Formed Steel Structures (1982: November 16-17; St. Louis, Missouri), Missouri S&T (formerly the University of Missouri - Rolla), 1982, pp. 45-74.

[12] Singer J., Arbocz J., Weller T., Buckling Experiments. Experimental methods in buckling of thin-walled structure. Basic concepts, columns, beams, and plates, John Wiley & Sons Inc. New York Volume 1, 1998, Volume 2, 2002.

[13] Tomblin J., Barbero E.J., Local buckling experiments on FRP columns, Thin-Walled Structures 18,1994, pp. 97-116.

[14] Barbero E.J., Trovillion J., Prediction and measurement of the post-critical behavior of fiber-reinforced composite columns, Composites Science and Technology 58, 1998, pp.1335-1341.

[15] Taheri F., Nagaraj M.and Khosravi P., Buckling response of glue-laminated columns reinforced with fiber-reinforced plastic sheets, Composite Structures 88, 2009, pp. 481–490.

[16] Wong P.M.H., Wang Y.C., An experimental study of pultruded glass fibre reinforced plastics channel columns at elevated temperatures, Composite Structures 81, 2007, pp. 84–95.

[17] Parlapalli M.R., Soh K.C., Shu D.W., Ma G., Experimental investigation of delamination buckling of stitched composite laminates, Composites: Part A 38 2007, pp. 2024–2033.

[18] Turvey G.J. and Zhang Y., A computational and experimental analysis of the buckling, postbuckling and initial failure of pultruded GRP columns, Computers and Structures 84, 2006, pp.1527–1537.